Hindawi
Advances in Civil Engineering
Volume 2019, Article ID 2143748, 9 pages
https://doi.org/10.1155/2019/2143748

Research Article

A Rheological Model of Sandstones considering Response to Thermal Treatment

Xingang Wang,[1] Lei Huang ,[2] and Junrong Zhang[3]

[1]*Department of Geology, Northwest University, Xi'an, Shanxi 710069, China*
[2]*Three Gorges Research Center for Geohazards, Ministry of Education, China University of Geosciences, Wuhan, Hubei 430074, China*
[3]*Department of Engineering Geology and Geotechnical Engineering, Faculty of Engineering, China University of Geosciences, Wuhan, Hubei 430074, China*

Correspondence should be addressed to Lei Huang; huanglei@cug.edu.cn

Received 24 December 2018; Revised 12 February 2019; Accepted 10 March 2019; Published 1 April 2019

Academic Editor: Zaobao Liu

Time-dependent rheological response of geomaterials to thermal treatment is a crucial issue in geothermal energy utilization and deep mineral mining. This response, however, has not yet been fully considered in the existing rheological constitutive models for sandstones. In order to experimentally investigate such responses and establish the associated rheological constitutive model, this study considers the sandstone specimens which have been thermally treated under different temperatures. The triaxial rheological test in conjunction with the scanning electron microscope is employed in the investigation to observe the mechanically and macro-/micromorphologically rheological response. Investigation results show that the thermal treatment induces microcracks and microdefects, and subsequently, they propagate during the creep. As a consequence, the heterogeneous deformation occurs, and macrocracks are present, leading to the irregular fluctuation and mutation in strain over time. A higher temperature contributes to a more severe structure damage and in turn reduces the intactness of sandstones and elevates the rheological response. The investigation allows successful establishment of a three-dimensional constitutive equation considering the instantaneous elastic response to thermal treatment. Based on the equation, a nonlinear visco-elastoplastic rheological constitutive model is developed for sandstones. Comparison with three existing rheological models shows that the model developed in this study could well represent the rheological process of the thermally treated sandstones.

1. Introduction

Thermal treatment plays an important role in the mechanical behaviors of rocks [1, 2]. It has also widely been reported that the engineering practices, such as the geothermal energy utilization and deep mineral mining, usually involve the rheological issue of thermally treated rocks [3, 4]. Because deep rocks are usually conditioned under high stress and long-term seepage pressure coupled with high temperature, it is of great interest to understand the rheological behavior of deep rocks in response to high-temperature thermal treatment [5, 6].

Recent advances in understanding the response of rocks or rock-like media to high-temperature thermal treatment include studies by Gautam et al. [7], Fan et al. [8], Yang et al. [9], Ersoy et al. [10], and Peng and Yang [11]. Among them, Gautam et al. [7] experimentally revealed that the elastic modulus of sandstones drops by 78% due to thermal treatment when the temperature rises from room temperature (25°C) to 650°C. Fan et al. [8] experimentally found that the temperature rise causes the decrease in wave velocity and Young's modulus of granites for the reason of thermal treatment. Yang et al. [9] observed the thermal damage of granites result from high temperature and showed the complicated response of multiple mechanical parameters (including strength, static elastic modulus, static Poisson's ratio, peak axial strain, dynamic elastic modulus, and dynamic Poisson's ratio) to the thermal treatment. Specifically, as temperature increases, the first two parameters rise, followed by their falling, while a falling in the static Poisson's

ratio is followed by its sharp rise, a continuing increase in the peak axial strain, and no significant change in the dynamic Poisson's ratio. As compared to the previous experiments, Ersoy et al. [10] performed the uniaxial compressive strength test of basic volcanic rocks under a wider range of temperature (200 to 1,000°C) and then revealed that the increasing temperature induces the thermal damage and in turn causes the strength loss. A wider range of rock types (sedimentary, metamorphic, and volcanic) was investigated in Peng and Yang [11], in which the continuing decrease in P wave velocity, compressive strength, and Young's modulus is observed as temperature increases, despite an exception occurrence at the three parameters of the quartz sandstones (increase initially and then decrease) due to high porosity. Numerous previous attentions have been paid to the response of various mechanical behaviors to thermal treatment, yet particular concerns are seldom placed on the rheological response. Investigations of the rheological response to thermal treatment, such as Belmokhtar et al. [5], are rare.

On the contrary, an increasing number of constitutive models have been developed to describe rock rheological behaviors in the past years. Chen et al. [12] reported a damage mechanism-based rheological model for granites with a consideration of thermal treatment. Xiong et al. [13] presented a unified thermo-elasto-viscoplastic rheological model for soft rocks in the critical state. Zhao et al. [14] developed a nonlinear elasto-viscoplastic rheological model with consideration of various deformation components. In the model, a parallel combination of Hooke and plastic slide bodies is incorporated, in conjunction with a Hooke body, a Kelvin body, and a generalized Bingham body. On the basis of variable-order fractional derivatives and continuum damage mechanics, Tang et al. [15] gave a four-element rheological model for salt rocks. Although continuing efforts have been devoted to the improvement of rock rheological constitutive models, the existing rheological constitutive models considering the rheological response to thermal treatment, such as the model of Chen et al. [12] for granites and the model of Yang et al. [16] for sandstones, are rare.

This work adds to the limited body of (1) investigation on the potential rheological response of sandstones to thermal treatment and (2) development of a rheological constitutive model for sandstones with proper consideration of such response. Initially, the sandstone specimens for the investigation are collected from the Majiagou rock slope located in the Three Gorges Reservoir area, in central China. Then, the specimens, separately, are thermally treated under different temperatures, prior to the triaxial rheological test for investigating the mechanically rheological response. In the test, the scanning electron microscope is employed to additionally investigate the micromorphologically rheological response. Based on the investigation of rheological response to thermal treatment, a three-dimensional constitutive equation is established by incorporating such response. A nonlinear visco-elastoplastic rheological constitutive model adopting this established equation is then developed for sandstones. At last, the estimates from the developed model are compared with that from the existing models and the laboratory observations to evaluate the performance of the developed model.

2. Laboratory Investigation of Rheological Response of Sandstones to Thermal Treatment

2.1. Materials and Methods

2.1.1. Preparation of Specimens and Description of Testing Instrument. The rock specimens are steel-gray fine sandstones. Their physical parameters are listed in Table 1. The cylindrical specimens to be tested were prepared with dimensions of $\Phi = 50$ mm and $H = 100$ mm.

The testing instrument, namely, triaxial rheometer, composed of the control system, oil source, axial compression system, confining pressure system, and seepage system along with sensors (shown in Figure 1), was employed. More details about the rheometer are available in Xu et al. [17]. In addition to the triaxial rheometer for observing the mechanically rheological response, a Quanta200 environmental scanning electron microscope is employed during the test to observe the micromorphologically rheological response.

2.1.2. Procedures of the Test. The following steps were adopted during the test:

(1) Select the rock specimens with close longitudinal wave velocities for the triaxial rheological test.

(2) Thermally treat the specimens under temperatures of 25°C (room temperature), 200°C, 400°C, and 600°C, separately, for 6 hours (h), prior to cooling down to the room temperature (shown in Figure 2). Due to time consumption of test, one specimen alone is prepared for each temperature above.

(3) Saturate the specimens for 24 h with the aid of the vacuum pump to ensure the full saturation before the triaxial rheological test.

(4) Conduct the triaxial rheological test using the triaxial rheometer. According to the field geostress, the confining pressure adopted in the triaxial rheological test is set at 6 MPa and the seepage pressure is set at 4 MPa. Deviatoric stress (the difference between axial pressure and confining pressure) loading is then imposed by grade. The loading duration under all levels of deviatoric stress is limited to be no less than 72 h, and the rate of deformation is limited to be no more than 0.001 mm/24 h. When the deformation becomes stable under the current level of deviatoric stress, then the next level is imposed. The test stops once the rock specimen is damaged. Note that, for sufficient contact between the specimen and rheometer, prior to graded loading, the preloading has been performed.

2.2. Investigation Results

2.2.1. Macromorphologically Rheological Response to Thermal Treatment. Figure 3 compares the macromorphology of 25, 200, 400, and 600°C thermally treated specimens after rheological failure. The 25°C thermally treated specimen after rheological failure presents an axial failure plane and

Table 1: Physical parameters of sandstone specimens.

Dry density (g/cm^3)	Natural density (g/cm^3)	Saturated density (g/cm^3)	Natural moisture content (%)	Saturated moisture content (%)	Porosity (%)	Longitudinal wave velocity (m/s)
2.58	2.62	2.67	0.59	1.06	7.5	2,813

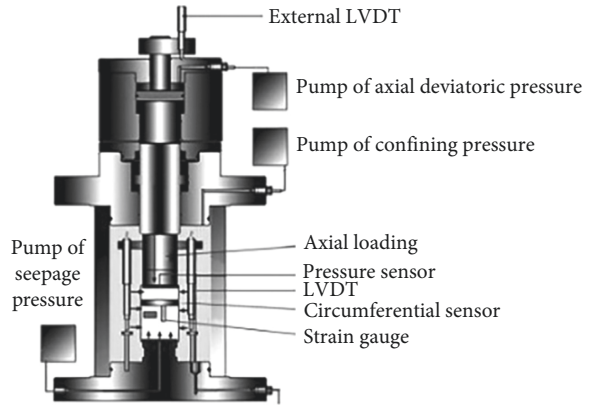

Figure 1: Triaxial rheometer [17]. Axial deformation was measured using two linear variable differential transformers (LVDTs) installed at the two sides of specimen, respectively.

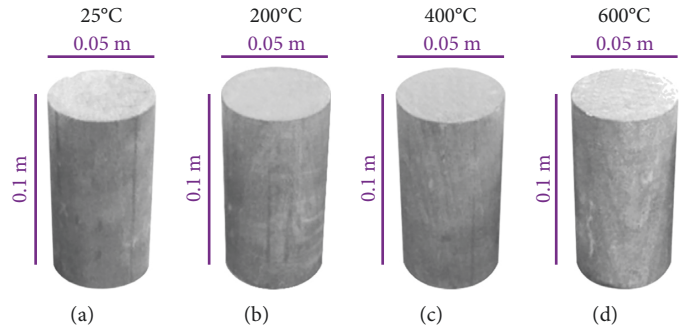

Figure 2: Thermally treated sandstone specimens before rheological failure.

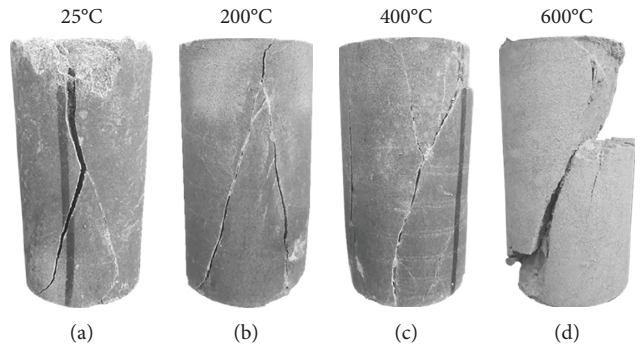

Figure 3: Sandstone specimens after rheological failure.

some cracks. The cracks are primarily tensile ones, supplemented by shear ones.

In comparison, the 200°C and 400°C thermally treated specimens after rheological failure presents a pair of X-shaped failure planes and some cracks. The cracks are primarily shear ones, supplemented by tensile ones. And the 600°C thermally treated specimen after rheological failure is crushed, and it presents an oblique failure plane. Numerous shear cracks are observed, and a large amount of powder is produced.

The comparison shows that the sandstones exhibit significant macromorphological rheological response to thermal treatment. A higher temperature contributes to a more severe structure damage and in turn reduces the intactness of sandstones.

2.2.2. Micromorphologically Rheological Response to Thermal Treatment. Figure 4 compares the microscopic morphology of failure planes of 25, 200, 400, and 600°C thermally treated specimens. The failure plane associated with 25°C is step-shaped, with each step being neat and smooth (shown in Figure 4(a)). The heights of steps vary from a few μm to 30 μm. In contrast, the failure planes associated with 200, 400, and 600°C are rough and irregularly shaped (shown in Figures 4(b)–4(d)). Loose structure, small sized particles, and holes are revealed.

This could be due to that thermal oxidation decomposition occurred under high temperature, and gas was produced. As a consequence, void was yielded within the sandstones. It could be hence inferred that a higher temperature renders a more severe rheological damage to sandstones.

2.2.3. Mechanically Rheological Response to Thermal Treatment. An example of the axial strain of thermally treated specimens over time is shown in Figure 5, accompanied with the change in instantaneous elastic modulus with the temperature used in thermal treatment. The instantaneous elastic modulus is determined using the following equation [9, 18]:

$$G_1 = \frac{\sigma_1 - \sigma_3}{3\left(\varepsilon_0 - \left(\left(\sigma_1 + 2\sigma_3\right)/9K\right)\right)}, \tag{1}$$

where G_1 is the instantaneous elastic modulus, σ_1 is the axial stress, σ_3 is the confining pressure, ε_0 is the instantaneous stain, and K is the bulk modulus.

In Figure 5(a), the strain sometimes exhibits slight fluctuation. As revealed in Figure 5(b), the instantaneous elastic modulus is significantly subject to the temperature used in thermal treatment. A higher temperature contributes to a smaller instantaneous elastic modulus value.

Figure 6 selects the axial strain and its rate over time during the last level of deviatoric stress loading. This figure shows that the sandstone experiences the following three rheological stages (ε is the axial strain, and $\ddot{\varepsilon}$ is the second derivative of ε):

(i) The deceleration rheological stage ($\ddot{\varepsilon} < 0$)

(ii) The stable rheological stage ($\ddot{\varepsilon} = 0$)

(iii) The acceleration rheological stage ($\ddot{\varepsilon} > 0$)

3. Developed Model considering Rheological Response to Thermal Treatment

Based on the investigation above of rheological response to thermal treatment, a three-dimensional constitutive equation is established here by incorporating such response. A nonlinear visco-elastoplastic rheological constitutive model adopting this established equation is then developed for sandstones.

3.1. Development of the Model

3.1.1. Identification of Instantaneous Elastic Response. Instantaneous elastic response of rocks to thermal treatment is normally quantified by an instantaneous elastic index, D, as defined by Kachanov [19]:

$$D = \frac{E_{\mathrm{M}}(0) - E_{\mathrm{K}}(0)}{E_{\mathrm{M}}(0)}, \tag{2}$$

where $E_{\mathrm{M}}(0)$ is the instantaneous elastic modulus before thermal treatment and $E_{\mathrm{K}}(0)$ is the instantaneous elastic modulus after thermal treatment.

The D ranges between 0 and 1. The investigation data in Section 2.2 give rise to the relation between D and the temperature (w) used in thermal treatment (Figure 7). As shown in this figure, D increases with w. A higher w value tends to result in a larger D value, signifying an elevated instantaneous elastic response of sandstones to thermal treatment. Fitting the data by the least square method gives

$$D = 0.49 - 0.56 \times e^{-(w/186.09)}. \tag{3}$$

3.1.2. Identification of Long-Term Rheology. Long-term rheological index, $D_{t_{\mathrm{D}}}$, as defined by Zhang et al. [20], is introduced to quantify the long-term rheology of sandstones:

$$D_{t_{\mathrm{D}}} = \frac{E_0 - E_{t_{\mathrm{D}}}}{E_0}, \tag{4}$$

where E_0 is the initial rheological viscoelastic coefficient or instantaneous elastic modulus of rock, t_{D} is the failure time point, and $E_{t_{\mathrm{D}}}$ is the rheological viscoelastic coefficient at t_{D}.

$E_{t_{\mathrm{D}}}$ tends to be a stable value (E_∞) under long-term seepage pressure. As stated by Zhou et al. [21], rock failure occurs in the situation where deviatoric stress is greater than the yield stress. Accordingly, t_{D} equivalently denotes the time point when the deviatoric stress starts to exceed the yield stress. Thus, equation (4) is rewritten as follows [20]:

$$D_{t_{\mathrm{D}}} = \frac{E_0 - E_\infty}{E_0}\left(1 - e^{-\alpha t_{\mathrm{D}}}\right), \tag{5}$$

where α is a coefficient related to damage tolerance.

3.1.3. Consideration of Instantaneous Elastic Response to Thermal Treatment and Long-Term Rheology into the Model. From Figures 5(a) and 6, the instantaneous elastic deformation (i.e., deceleration rheological stage) of the thermally treated sandstone occurs once the axial stress is loaded, indicating that the rheological model should contain a series-wound elastic element. In the stable rheological stage, the strain under a low level of deviatoric stress tends to be constant, which suggests that the rheological model should include an adhesive element and an elastic element in parallel. In comparison, under a high level of deviatoric

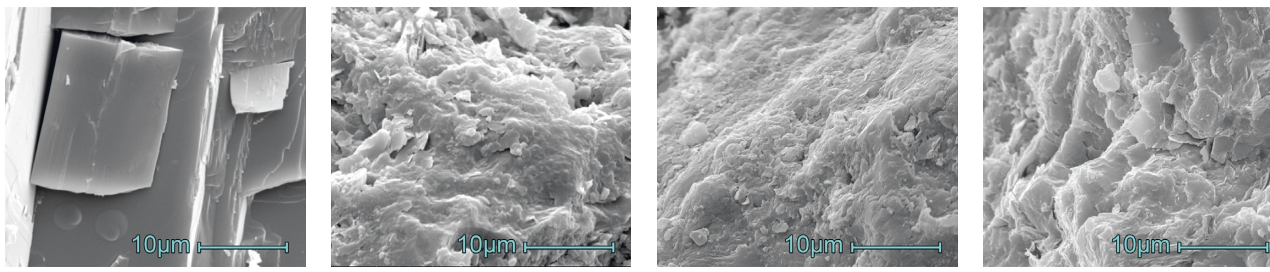

(a) (b) (c) (d)

Figure 4: The micromorphology of sandstone specimens after rheological failure under the environmental scanning electron microscope. Before the rheological test, the specimens have experienced thermal treatment under the temperature of (a) 25°C, (b) 200°C, (c) 400°C, and (d) 600°C, respectively.

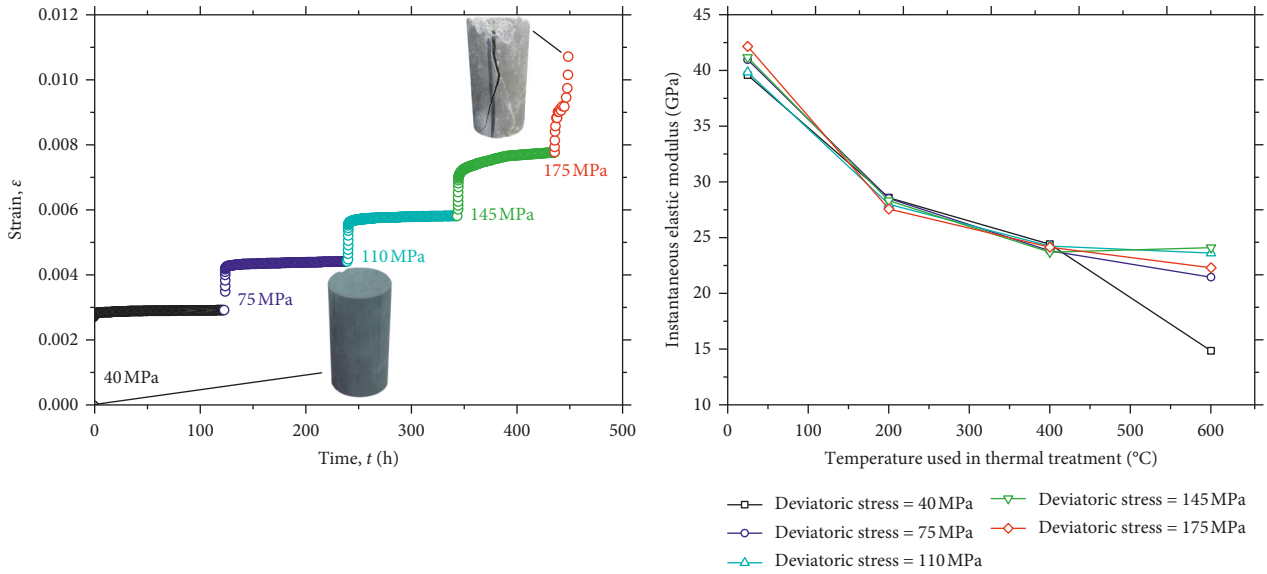

(a) (b)

Figure 5: (a) Axial strain over time. (b) Instantaneous elastic modulus against temperature used in thermal treatment.

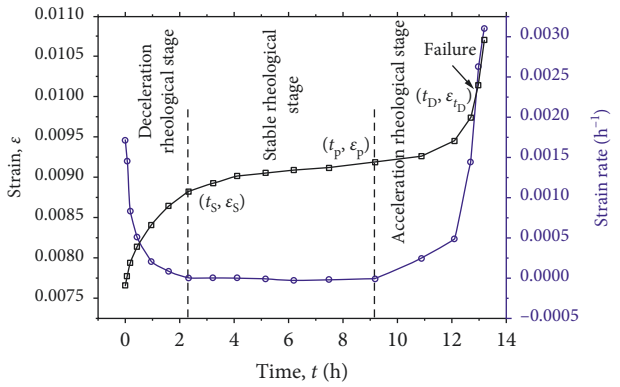

Figure 6: Axial strain and its rate over time (temperature = 25°C, deviatoric stress = 175 MPa). t_s is the time point of conversion from the deceleration rheological stage to stable rheological stage, ε_s is the strain at t_s, t_p is the time point of conversion from the stable rheological stage to acceleration rheological stage, ε_p is the strain at t_p, t_D is the the failure time point, and ε_{t_D} is the strain at t_D.

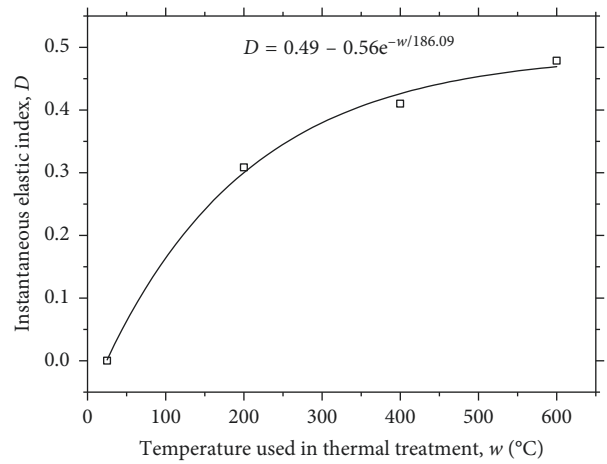

Figure 7: Instantaneous elastic index against temperature used in thermal treatment.

stress, the strain increases with time, which implies that a plastic component should be included in the rheological model. In the acceleration rheological stage, the deformation increases sharply with time, indicating nonlinearity. It suggests that the rheological model should include a nonlinear viscous element.

Based on the analysis above, a nonlinear visco-elastoplastic rheological model, as shown in Figure 8, is developed. The model is composed of (1) a Hook element, (2) a Kelvin–Voigt element, (3) a visco-elastoplastic body, and (4) a nonlinear viscous body. The instantaneous elastic index D defined by Kachanov [19] has been introduced into model so as to consider the rheological response of sandstones to thermal treatment. Also, the long-term rheological index D_{t_D} defined by Zhang et al. [20] has been introduced to consider the long-term rheology.

The nonlinear viscous body used in the developed model is the parallel combination of a nonlinear Newton body and a plastic body. The constitutive equation for the Newton body can be expressed as follows:

$$\varepsilon = \frac{\sigma}{\eta}, \tag{6}$$

where σ is the total stress, ε is the total strain, and η is the viscous coefficient.

Denote

$$\eta = \eta_3 (t-a)^2, \tag{7}$$

where η_3 is the coefficient of the acceleration rheological initial viscosity and a is determined by the rheological curve fitting.

Substituting equation (7) to equation (6) gives

$$\varepsilon = \frac{\sigma}{\eta_3 (t-a)^2}. \tag{8}$$

Elastic modulus, E, can be expressed as

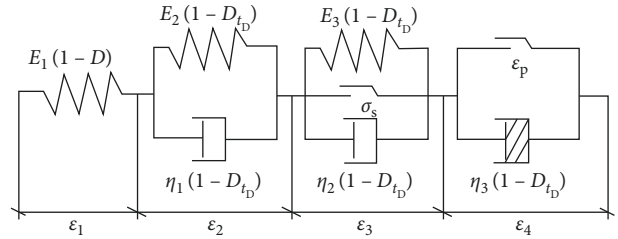

Figure 8: The developed model. E_1 is the instantaneous elastic modulus; E_2 and E_3 are viscoelasticity modules; η_1, η_2, and η_3 are coefficients of viscoelasticity; ε_1, ε_2, ε_3, and ε_4 are the strains of individual rheology bodies; and σ_s is the yield stress, which is determined by the conventional triaxial compression test.

$$E = E_0\left(1 - D_{t_D}\right). \tag{9}$$

Substituting equation (5) to equation (9) gives

$$E = E_0 e^{-\alpha t} + E_\infty\left(1 - e^{-\alpha t_D}\right). \tag{10}$$

Similarly, viscous coefficient, η (for the constitutive bodies other than the Newton body), can be expressed as

$$\eta = \eta_0\left(1 - D_{t_D}\right), \tag{11}$$

where η_0 is the initial viscosity coefficient.

Substituting equation (5) to equation (11) gives

$$\eta(t) = \eta_0 \frac{E_0 e^{-\alpha t} + E_\infty\left(1 - e^{-\alpha t_D}\right)}{E_0}. \tag{12}$$

In the conventional triaxial test, the stress status is $\sigma_2 = \sigma_3$. The stress status and load σ_1 of each level are constant after loading. Accordingly, the three-dimensional rheological equation of nonlinear visco-elastoplastic rheological model which considers the rheological response of sandstones to thermal treatment is shown as follows:

$$\varepsilon = \begin{cases} \dfrac{\sigma_1 + 2\sigma_3}{9K} + \dfrac{\sigma_1 - \sigma_3}{3G_1(1-D)} + \dfrac{\sigma_1 - \sigma_3}{3G_2}\left(1 - e^{-(G_2/\eta_1)t}\right), & \text{if } \sigma_1 - \sigma_3 \le \sigma_S, \\ \dfrac{\sigma_1 + 2\sigma_3}{9K} + \dfrac{\sigma_1 - \sigma_3}{3G_1(1-D)} + \dfrac{\sigma_1 - \sigma_3}{3G_2\left(1 - D_{t_D}\right)}\left(1 - e^{-(G_2/\eta_1)t}\right) + \dfrac{\sigma_1 - \sigma_3 - \sigma_S}{3G_3\left(1 - D_{t_D}\right)}\left(1 - e^{-(G_3/\eta_2)t}\right), & \text{if } \sigma_1 - \sigma_3 \ge \sigma_S \text{ and } \varepsilon \le \varepsilon_P, \\ \dfrac{\sigma_1 + 2\sigma_3}{9K} + \dfrac{\sigma_1 - \sigma_3}{3G_1(1-D)} + \dfrac{\sigma_1 - \sigma_3}{3G_2\left(1 - D_{t_D}\right)}\left(1 - e^{-(G_2/\eta_1)t}\right) & \\ \quad + \dfrac{\sigma_1 - \sigma_3 - \sigma_S}{3G_3\left(1 - D_{t_D}\right)}\left(1 - e^{-(G_3/\eta_2)t}\right) + \dfrac{\sigma_1 - \sigma_3}{3\eta_3\left(1 - D_{t_D}\right)(t-a)^2}, & \text{if } \sigma_1 - \sigma_3 \ge \sigma_S \text{ and } \varepsilon \ge \varepsilon_P, \end{cases} \tag{13}$$

where K is the bulk modulus and G_1, G_2, and G_3 are the shear modulus, respectively, corresponding to E_1, E_2, and E_3 in the three-dimensional stress state. The four parameters K, G_1, G_2, and G_3 can be determined as follows [22]:

$$\begin{cases} K = \dfrac{E}{3(1-2\mu)}, \\ G_i = \dfrac{E_i}{2(1+\mu)}, \quad i = 1, 2, 3. \end{cases} \tag{14}$$

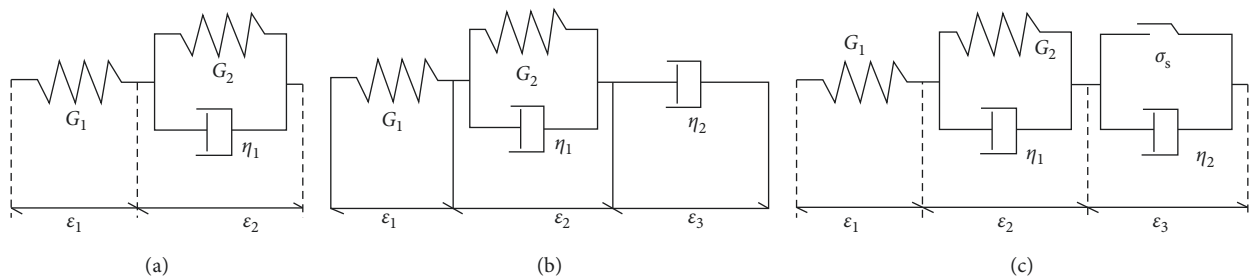

Figure 9: The existing models: (a) Kelvin–Voigt model; (b) Burgers model; (c) Nishihara model.

Table 2: Parameters of the developed rheological model and the existing models.

Model	Deviatoric stress (MPa)	G_1 (GPa)	G_2 (GPa)	G_3 (GPa)	η_1 (GPa·h)	η_2 (GPa·h)	η_3 (GPa·h)	a	R^2
The developed model	40	39.6	66.63	N/A	58.15	N/A	N/A	N/A	0.86
	75	40.98	28.83	N/A	1.11	N/A	N/A	N/A	0.83
	110	39.86	33.82	N/A	7.889	N/A	N/A	N/A	0.85
	145	41.19	44.81	7.48	2.27	20.36	N/A	N/A	0.99
	175	42.17	147.58	13.38	40.24	33.096	N/A	N/A	0.99
	175*	42.17	147.58	13.38	40.24	33.09	16.24	13.96	0.99
Kelvin–Voigt model	175	42.17	25.24	N/A	130.75	N/A	N/A	N/A	0.72
Burgers model	175	42.17	80.58	N/A	42.03	1500.49	N/A	N/A	0.78
Nishihara model	175	42.17	80.41	N/A	35.11	257.68	N/A	N/A	0.81

N/A: not applicable; *during the acceleration rheological stage.

As mentioned in Section 2.1.2, prior to graded loading, the preloading has been performed. As is known, the preloading would result in some creep. This creep resulting from the low preloading pressure acted, however, would be rather small so that the influence of such creep could be even ignored [23, 24]. For this reason, the creep due to preloading is not considered into the developed model.

3.2. Performance of the Developed Model. In this section, the estimates from the developed model are compared with that from the existing models and the laboratory observations to evaluate the performance of the developed model. The existing models selected to compare includes the following:

(i) The Kelvin–Voigt model [25, 26] (Figure 9(a))

(ii) The Burgers model [27, 28] (Figure 9(b))

(iii) The Nishihara model [29, 30] (Figure 9(c)).

In order to obtain the parameter values of the developed model and the existing models, the rheological test data are processed through the Boltzmann superposition principle (Sone and Zoback [31]) first. Then, the data are fitted to the models, with the fitted model parameter values listed in Table 2. The developed model and the existing models adopting the respective parameters are thus established.

The estimates from the developed model and the laboratory observations are compared in Figure 10. The comparison shows that the estimate from the developed model is consistent with the sandstone triaxial rheological test result.

The estimates from the developed model and that from the selected existing models are compared in Figure 11. Figure 11 demonstrates that the developed model better reflects the rheological process of the thermally treated sandstones in comparison with the Kelvin–Voigt model, the Burgers model, and the Nishihara model.

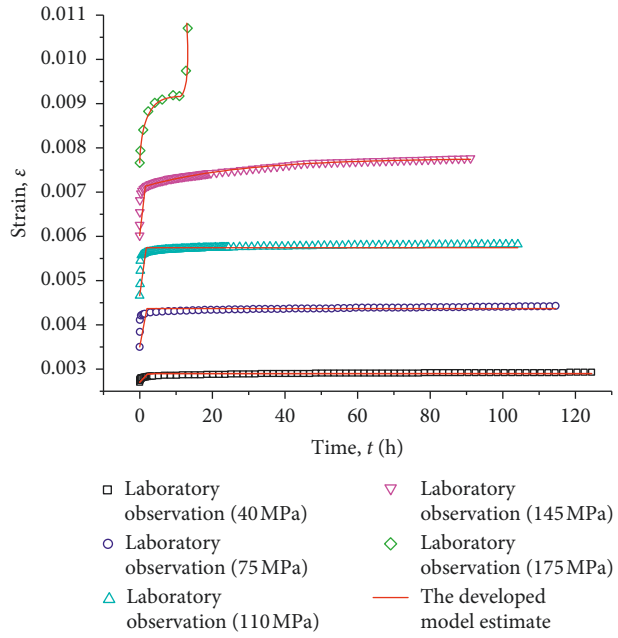

Figure 10: Comparison of axial strains from the laboratory observation and the developed model estimate.

4. Conclusions

This work adds to the limited body of (1) investigation on the potential rheological response (mechanically and macro-/

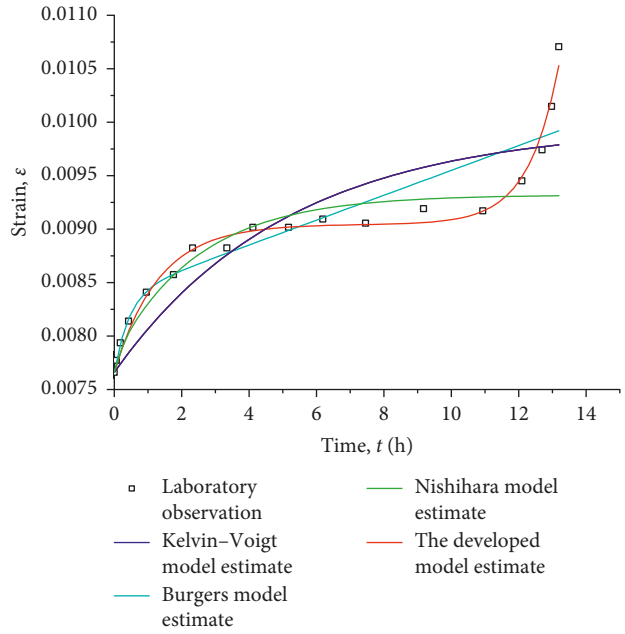

Figure 11: Comparison of axial strain estimates from the existing models and the developed model.

micromorphologically) of sandstones to thermal treatment and (2) development of a rheological model for sandstones with proper consideration of such response.

Investigation results show that the thermal treatment induces microcracks and microdefects, and subsequently, they propagate during the creep. As a consequence, the heterogeneous deformation occurs and macrocracks are present, leading to the irregular fluctuation and mutation in strain over time. A higher temperature contributes to a more severe structure damage and in turn reduces the intactness of sandstones and elevates the rheological response.

Based on the investigation of rheological response to thermal treatment, a three-dimensional constitutive equation is established by incorporating such response. A nonlinear visco-elastoplastic rheological model adopting this established equation is then developed for sandstones. In comparison with the existing models, the developed model shows a better fit with the triaxial rheological test observations, revealing the capability to represent the rheological process of the thermally treated sandstones. The developed model can serve for numerical simulation as the constitutive model.

Data Availability

The data used to support the findings of this study are included within the article.

Conflicts of Interest

The authors declare that they have no conflicts of interest.

Acknowledgments

The research was supported by two funds, namely, the Open Fund Project of Key Laboratory for Geo-Hazards in Loess Area of China (Grant no. KLGLAMLR201505) and the Open Foundation of Jiangxi Engineering Research Center of Water Engineering Safety and Resources Efficient Utilization (Grant no. OF201602).

References

[1] S. Raude, F. Laigle, R. Giot, and R. Fernandes, "A unified thermoplastic/viscoplastic constitutive model for geomaterials," *Acta Geotechnica*, vol. 11, no. 4, pp. 849–869, 2016.

[2] X. Nie, X. Wei, X. Li, and C. Lu, "Heat treatment and ventilation optimization in a deep mine," *Advances in Civil Engineering*, vol. 2018, Article ID 1529490, 12 pages, 2018.

[3] G. Fabre and F. Pellet, "Creep and time-dependent damage in argillaceous rocks," *International Journal of Rock Mechanics and Mining Sciences*, vol. 43, no. 6, pp. 950–960, 2006.

[4] L. L. N. Mambou, J. Ndop, and J. M. B. Ndjaka, "Theoretical investigations of mechanical properties of sandstone rock specimen at high temperatures," *Journal of Mining Science*, vol. 50, no. 1, pp. 69–80, 2014.

[5] M. Belmokhtar, P. Delage, S. Ghabezloo, and N. Conil, "Thermal volume changes and creep in the callovo-oxfordian claystone," *Rock Mechanics and Rock Engineering*, vol. 50, no. 9, pp. 2297–2309, 2017.

[6] I. Tomac and M. Sauter, "A review on challenges in the assessment of geomechanical rock performance for deep geothermal reservoir development," *Renewable and Sustainable Energy Reviews*, vol. 82, pp. 3972–3980, 2018.

[7] P. K. Gautam, A. K. Verma, M. K. Jha, K. Sarkar, T. N. Singh, and R. K. Bajpai, "Study of strain rate and thermal damage of Dholpur sandstone at elevated temperature," *Rock Mechanics and Rock Engineering*, vol. 49, no. 9, pp. 3805–3815, 2016.

[8] L. F. Fan, Z. J. Wu, Z. Wan, and J. W. Gao, "Experimental investigation of thermal effects on dynamic behavior of granite," *Applied Thermal Engineering*, vol. 125, pp. 94–103, 2017.

[9] S.-Q. Yang, P. G. Ranjith, H.-W. Jing, W.-L. Tian, and Y. Ju, "An experimental investigation on thermal damage and failure mechanical behavior of granite after exposure to different high temperature treatments," *Geothermics*, vol. 65, pp. 180–197, 2017.

[10] H. Ersoy, H. Kolaylı, M. Karahan, H. H. Karahan, and M. O. Sünnetci, "Effect of thermal damage on mineralogical and strength properties of basic volcanic rocks exposed to high temperatures," *Bulletin of Engineering Geology and the Environment*, vol. 78, no. 3, pp. 1515–1525, 2019.

[11] J. Peng and S.-Q. Yang, "Comparison of mechanical behavior and acoustic emission characteristics of three thermally-damaged rocks," *Energies*, vol. 11, no. 9, p. 2350, 2018.

[12] L. Chen, C. P. Wang, J. F. Liu et al., "A damage-mechanism-based creep model considering temperature effect in granite," *Mechanics Research Communications*, vol. 56, pp. 76–82, 2014.

[13] Y.-L. Xiong, G.-L. Ye, H.-H. Zhu, S. Zhang, and F. Zhang, "A unified thermo-elasto-viscoplastic model for soft rock," *International Journal of Rock Mechanics and Mining Sciences*, vol. 93, pp. 1–12, 2017.

[14] Y. Zhao, Y. Wang, W. Wang, W. Wan, and J. Tang, "Modeling of non-linear rheological behavior of hard rock using triaxial rheological experiment," *International Journal of Rock Mechanics and Mining Sciences*, vol. 93, pp. 66–75, 2017.

[15] H. Tang, D. Wang, R. Huang, X. Pei, and W. Chen, "A new rock creep model based on variable-order fractional derivatives and continuum damage mechanics," *Bulletin of Engineering Geology and the Environment*, vol. 77, no. 1, pp. 375–383, 2018.

[16] S.-Q. Yang, B. Hu, P. Ranjith, and P. Xu, "Multi-step loading creep behavior of red sandstone after thermal treatments and a creep damage model," *Energies*, vol. 11, no. 1, p. 212, 2018.
[17] W.-Y. Xu, R.-B. Wang, W. Wang, Z.-L. Zhang, J.-C. Zhang, and W.-Y. Wang, "Creep properties and permeability evolution in triaxial rheological tests of hard rock in dam foundation," *Journal of Central South University*, vol. 19, no. 1, pp. 252–261, 2012.
[18] Y. Li and C. Xia, "Time-dependent tests on intact rocks in uniaxial compression," *International Journal of Rock Mechanics and Mining Sciences*, vol. 37, no. 3, pp. 467–475, 2000.
[19] L. Kachanov, "Crack and damage growth in creep—a combined approach," *International Journal of Fracture*, vol. 16, no. 4, pp. 179–181, 1980.
[20] Q. Y. Zhang, W. D. Yang, J. G. Zhang et al., "Variable parameters-based creep damage constitutive model and its engineering application," *Chinese Journal of Rock Mechanics and Engineering*, vol. 28, no. 4, pp. 732–739, 2009.
[21] H. W. Zhou, C. P. Wang, B. B. Han, and Z. Q. Duan, "A creep constitutive model for salt rock based on fractional derivatives," *International Journal of Rock Mechanics and Mining Sciences*, vol. 48, no. 1, pp. 116–121, 2011.
[22] X. Wang, Y. Yin, J. Wang, B. Lian, H. Qiu, and T. Gu, "A nonstationary parameter model for the sandstone creep tests," *Landslides*, vol. 15, no. 7, pp. 1377–1389, 2018.
[23] H. Zhang, Z. Wang, Y. Zheng, P. Duan, and S. Ding, "Study on tri-axial creep experiment and constitutive relation of different rock salt," *Safety Science*, vol. 50, no. 4, pp. 801–805, 2012.
[24] L. Gao, W. Lin, D. Sun, and H. Wang, "Experimental anelastic strain recovery compliance of three typical rocks," *Rock Mechanics and Rock Engineering*, vol. 47, no. 6, pp. 1987–1995, 2014.
[25] R. E. Hutter and S. Green, "Quantifying creep behaviour of clay-bearing rocks below the critical stress state for rapid failure: mam tor landslide, Derbyshire, England," *Journal of the Geological Society*, vol. 168, no. 2, pp. 359–372, 2011.
[26] B. Nedjar and R. Le Roy, "An approach to the modeling of viscoelastic damage: application to the long-term creep of gypsum rock materials," *International Journal for Numerical and Analytical Methods in Geomechanics*, vol. 37, no. 9, pp. 1066–1078, 2013.
[27] W. Korzeniowski, "Rheological model of hard rock pillar," *Rock Mechanics and Rock Engineering*, vol. 24, no. 3, pp. 155–166, 1991.
[28] P. Nomikos, R. Rahmannejad, and A. Sofianos, "Supported axisymmetric tunnels within linear viscoelastic burgers rocks," *Rock Mechanics and Rock Engineering*, vol. 44, no. 5, pp. 553–564, 2011.
[29] M. Nishihara, "Creep of shale and sandy-shale," *Journal of the Geological Society of Japan*, vol. 58, no. 683, pp. 373–377, 1952.
[30] S.-W. Hao, B.-J. Zhang, J.-F. Tian, and D. Elsworth, "Predicting time-to-failure in rock extrapolated from secondary creep," *Journal of Geophysical Research: Solid Earth*, vol. 119, no. 3, pp. 1942–1953, 2014.
[31] H. Sone and M. D. Zoback, "Time-dependent deformation of shale gas reservoir rocks and its long-term effect on the in situ state of stress," *International Journal of Rock Mechanics and Mining Sciences*, vol. 69, pp. 120–132, 2014.